Water magnetic relaxation dispersion in biological systems: The contribution of proton exchange and implications for the noninvasive detection of cartilage degradation

Umamaheswar Duvvuri*†, Ari D. Goldberg*, James K. Kranz‡, Linh Hoang‡, Ravinder Reddy*, Felix W. Wehrli*, A. Joshua Wand‡, S. W. Englander‡, and John S. Leigh*

Departments of *Radiology and ‡Biochemistry and Biophysics, Metabolic Magnetic Resonance Research and Computing Center, University of Pennsylvania, Philadelphia, PA 19104

Contributed by S. W. Englander, September 5, 2001

Magnetic relaxation has been used extensively to study and characterize biological tissues. In particular, spin-lattice relaxation in the rotating frame ($T_{1\rho}$) of water in protein solutions has been demonstrated to be sensitive to macromolecular weight and composition. However, the nature of the contribution from low frequency processes to water relaxation remains unclear. We have examined this problem by studying the water $T_{1\rho}$ dispersion in peptide solutions (^{14}N- and ^{15}N-labeled), glycosaminoglycan solutions, and samples of bovine articular cartilage before and after proteoglycan degradation. We find in model systems and tissue that hydrogen exchange from NH and OH groups to water dominates the low frequency water $T_{1\rho}$ dispersion, in the context of the model used to interpret the relaxation data. Further, low frequency dispersion changes are correlated with loss of proteoglycan from the extra-cellular matrix of articular cartilage. This finding has significance for the noninvasive detection of matrix degradation.

rotating frame | $T_{1\rho}$ | extra-cellular matrix | osteoarthritis

Protein degradation with a loss of proteoglycan (PG) from the extra-cellular matrix is thought to be an initiating event of early osteoarthritis (1). A noninvasive imaging method that can monitor the progression of the disease would be highly desirable for the longitudinal evaluation of disease progression and the utility of therapeutic interventions. Because of the excellent soft tissue contrast and its noninvasive nature, MRI is an attractive modality for imaging cartilage. Unfortunately, currently available conventional MRI methods are unable to detect the earliest stages of the disease when biochemical changes occur without gross tissue damage (2). Recently, several MRI methods have been proposed to detect PG loss from cartilage (3, 4). In particular, spin-lattice relaxation in the rotating frame ($T_{1\rho}$) has been demonstrated to be elevated in PG-depleted cartilage (5).

$T_{1\rho}$ relaxation is sensitive to molecular motions that have correlation times (τ) such that $\tau\omega_{SL}\sim1$, where $\omega_{SL} = \gamma B_{SL}$ is the strength of the spin-lock field (6). $T_{1\rho}$ increases with the strength of the spin-lock field, a phenomenon termed dispersion. $T_{1\rho}$ measurements can therefore provide information about the biophysical mechanisms underlying magnetic relaxation. It has been demonstrated that water $T_{1\rho}$ relaxation and dispersion (in the 0.1–10 kHz regime) are sensitive to macromolecule–water interactions in protein solutions and possibly also in biological tissues (7–9). Low frequency (0.1–3 kHz) $T_{1\rho}$ dispersion has been observed in several systems such as protein solutions (7), bovine articular cartilage (5), human patellar cartilage (10), rodent brain (11), and murine tumor tissue (9). However, the exact nature of $T_{1\rho}$ dispersion in biological tissues remains unclear. The range of spin-lock strengths that can be used for *in vivo* measurements is 0.1–3 kHz (depending on the duration of the spin-lock pulse), without exceeding power deposition limits. Therefore, we have focused our investigations on the low frequency dispersion in biological systems. The goal of this work is to investigate the biophysical mechanisms underlying $T_{1\rho}$ relaxation in biological tissues. Such experiments may help to improve existing MRI methods and provide a basis for the quantitative interpretation of relaxation in normal and diseased cartilage.

Proton exchange between chemically shifted NH and OH groups and the solvent water, along with quadrupolar relaxation effects of the ^{14}N (spin = 1) and ^{17}O (spin = 5/2) modulated by the scalar coupling and proton exchange, contribute to the observed low frequency water $T_{1\rho}$ relaxation in articular cartilage. We have investigated these potential mechanisms underlying bulk water $T_{1\rho}$ dispersion by studying peptide solutions (a model for protein in cartilage), chondroitin sulfate (CS) type C solutions (a major component of cartilage PG), and bovine articular cartilage before and after sequential PG depletion. By using an unstructured polypeptide with many exchangeable NH protons but few hydroxyl groups, the effects of NH groups on water $T_{1\rho}$ dispersion were studied. ^{15}N- to ^{14}N-isotope substitution experiments were performed to determine the effect of ^{14}N quadrupolar relaxation on bulk water relaxation. The effects of hydroxyl group exchange were investigated by measuring the $T_{1\rho}$ dispersion of CS solutions, which have many exchangeable OH groups. These data were used to give some general interpretations for the observed $T_{1\rho}$ dispersion profile of normal and PG-depleted cartilage.

Methods

Measurements on Model Solutions. All NMR experiments were performed on a 2T magnet interfaced to a custom-built console at room temperature (22°C), unless otherwise stated. A 1-cm diameter solenoidal coil tuned to 86 MHz was used. Spectroscopic relaxation rates of water were measured as described (5). Water proton T_1 was measured with an inversion recovery sequence [repetition time (TR) = 12 s, 1,024 data points, 5 kHz bandwidth, with 20 free induction decays (FIDs)], and the inversion time was varied from 400–8,000 ms in steps of 400 ms. $T_{1\rho}$ relaxation times were measured with a spin-locking sequence, with the length of the spin-lock pulse varied between 0.5–10 s in increments of 0.5 s, and the TR time was set to be greater than 5 T_1 s. All other parameters were as given previ-

Abbreviations: $T_{1\rho}$, spin-lattice relaxation in the rotating frame; PG, proteoglycan; CS, chondroitin sulfate; smMLCKp, smooth muscle myosin light-chain kinase peptide from chicken.

†To whom reprint requests should be addressed at: B-1 Stellar-Chance Labs, Department of Radiology, Magnetic Resonance Research and Computing Center, University of Pennsylvania, Philadelphia, PA 19104-6100. E-mail: uduvvuri@mail.med.upenn.edu.

The publication costs of this article were defrayed in part by page charge payment. This article must therefore be hereby marked "*advertisement*" in accordance with 18 U.S.C. §1734 solely to indicate this fact.

ously. $T_{1\rho}$ dispersion was characterized by varying the amplitude of the spin-lock pulse. Phosphate buffer (200 mM, pH 7.4) was used for all peptide NMR experiments. Polyethylene glycol (PEG) [average molecular weight = 1,450; 0.1% wt/vol (pH 7.4); Sigma] has no exchangeable protons, thus it provides a convenient control to determine the effects of proton exchange on $T_{1\rho}$ dispersion.

The peptide based on the calmodulin-binding domain of smooth muscle myosin light-chain kinase peptide from chicken [smMLCKp (GSARRKWQKTGHAVRAIGRLS)] was prepared as described in *Escherichia coli* BL21(DE3) cells (12). ^{15}N-labeled peptide was prepared from *E. coli* grown on minimal media with $^{15}NH_4Cl$ as the only nitrogen source. Peptide solution purity was 99.9% (HPLC analysis). For NMR, the peptide was in phosphate buffer at the desired concentration.

CS type C was obtained from Sigma and used without further purification. CS solutions of various concentrations (2, 5, and 10% wt/vol) were in PBS (137 mM NaCl/2.7 mM KCl/10 mM phosphate, pH 7.4; Sigma). Collagen type II, from bovine Achilles tendon (Sigma), was used without further purification to make collagen suspensions (10% wt/vol) in PBS.

Measurements on Bovine Cartilage. Bovine patellae were obtained from a local butcher. Cartilage discs (9-mm diameter) were cored from the articular surface of the patellae, underlying bone was removed, and the tissue was placed in PBS on ice for 2 h before NMR measurements. Enzymatic digestion was performed with trypsin (0.1 mg/ml; Sigma) at 26°C in PBS at pH 7.4. $T_{1\rho}$ dispersion profiles of bovine articular cartilage were measured before and after enzymatic digestion. The loss of PG from the extra-cellular matrix of the tissue was determined by the spectrophotometric assay of Frandale *et al.* (13). Any collagen loss induced by the trypsin digestion was determined according to the analysis of Bank *et al.* (14). $T_{1\rho}$ measurements used repetition time (TR) = 5 s, and the length of the spin-lock pulse varied from 20–600 ms in 30 equal increments. T_1 measurements used a standard inversion-recovery sequence (TR = 6 s, 1,024 data points, 5 kHz bandwidth, 20 free induction decays); different interpulse delays were used to compute T_1 values.

Relaxation times were determined by fitting the signal amplitude to a monoexponential decay as a function of the spin-locking time. The dispersion analysis was performed by fitting the relaxation rate ($R_{1\rho} = T_{1\rho}^{-1}$) as a function of the spin-lock pulse strength (ω_{SL}) according to the following Lorentzian equation:

$$R_{1\rho}(\omega_{SL}) = \left(\frac{A}{1 + \omega_{SL}^2\tau_{obs}^2}\right) + B, \qquad [1]$$

where A and B are constants, and τ_{obs} is the effective correlation time for $T_{1\rho}$ dispersion. This function describes the spectral character of any stochastic process and is maximized when $\omega_{SL}\tau_{obs} \approx 1$. This empirical function assumes that chemical exchange influences dispersion with an exponential autocorrelation function. A similar expression was shown to be applicable to relaxation caused by proton exchange (15). Dispersion profiles from cartilage were fit to a bi-Lorentzian function.

Results

Water $R_{1\rho}$ dispersion increased with the smMLCKp peptide concentration (Fig. 1). Isotopic substitution of ^{15}N for ^{14}N in the peptide reduced the $R_{1\rho}$ dispersion by only 10%, indicating that the effect of ^{14}N quadrupolar relaxation on water is small at physiologic pH in this peptide system. The effective correlation time (τ_{obs}) that characterizes the dispersion was 0.58 ms, yielding a rate of $\approx$1,700 s^{-1} (Eq. **1**). To test whether this dispersion was caused by a viscosity effect, the $R_{1\rho}$ dispersion of a polyethylene glycol (PEG) solution (0.1% wt/vol) was also measured and found not to increase dispersion (data not shown).

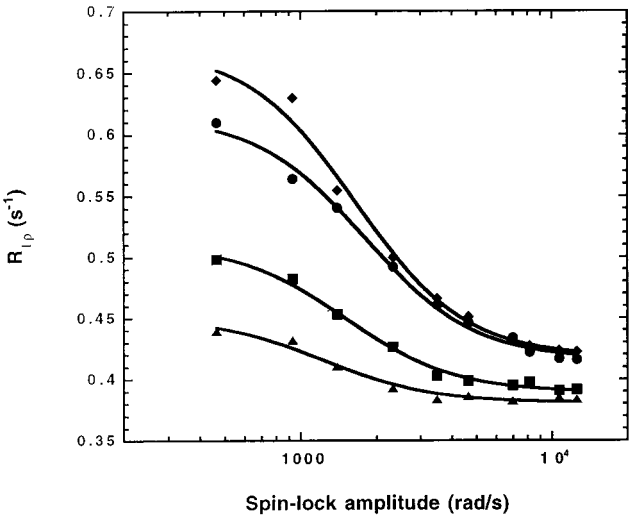

Fig. 1. Dependence of water $R_{1\rho}$ dispersion on peptide concentration. The dispersion of the buffer (▲), attributed to natural abundance $H_2{}^{17}O$ effects, increases in 0.9 mM ^{14}N-peptide solution (■) and 1.6 mM ^{14}N-peptide solution (◆). The dispersion of the 1.6 mM ^{15}N-peptide solution (●) is only 10% less than that of 1.6 mM ^{14}N-peptide solution, indicating that ^{14}N relaxation is not the dominant mechanism modulating the interaction between NH and water protons.

The dependence of $R_{1\rho}$ on solute concentration was also established with CS solutions (Fig. 2). The amplitude of the dispersion curve increased with the CS concentration. The effective correlation rate associated with water dispersion in the CS solutions was $\approx$1,200 s^{-1}. It is evident that all of the curves do not asymptote to the same value. This shift in relaxation rate at high spin-lock fields is attributed to changes in T_1 relaxation associated with increased concentrations of CS. Water $R_{1\rho}$ was found to linearly depend on CS concentration *in vitro* (Fig. 2*B*). The magnitude of this dependence varied with the used spin-lock amplitude, indicating that the relaxation effect of CS on water is frequency-dependent.

In contrast to the model systems described hitherto, the water $R_{1\rho}$ dispersion profile of bovine articular cartilage was best described with a bi-Lorentzian function in the 0.1–2 kHz frequency range (Fig. 3). The parameters that characterize the dispersion profile before and after degradation are given in Table 1. The change in the slow correlation time, obtained by pooling the data from 5 samples each degraded through 3 sequential digestions (giving 15 data points), correlated with PG loss ($P < 0.005$, $r = -0.74$, Spearman's product moment correlation). The dispersion profile of the collagen suspension was also better characterized by a bi-Lorentzian than a single Lorentzian function (data not shown).

Hydroxyproline was extruded into the digestion media after 1 h of trypsin digestion, presumably from collagen degradation. Subsequent digestion did not significantly increase collagen loss ($P = 0.13$). These data indicate that trypsin treatment caused only a minimal initial loss of collagen from the tissue. It is interesting to note that although the entire dispersion curve seems to be uniformly altered after the initial digestion (in which both PG and collagen were depleted), only the low frequency dispersion component is altered on subsequent digestion (in which PG was lost but collagen content was maintained).

Discussion

Despite ongoing research efforts, there is no consensus view of water relaxation in biological systems (16, 17). There are several

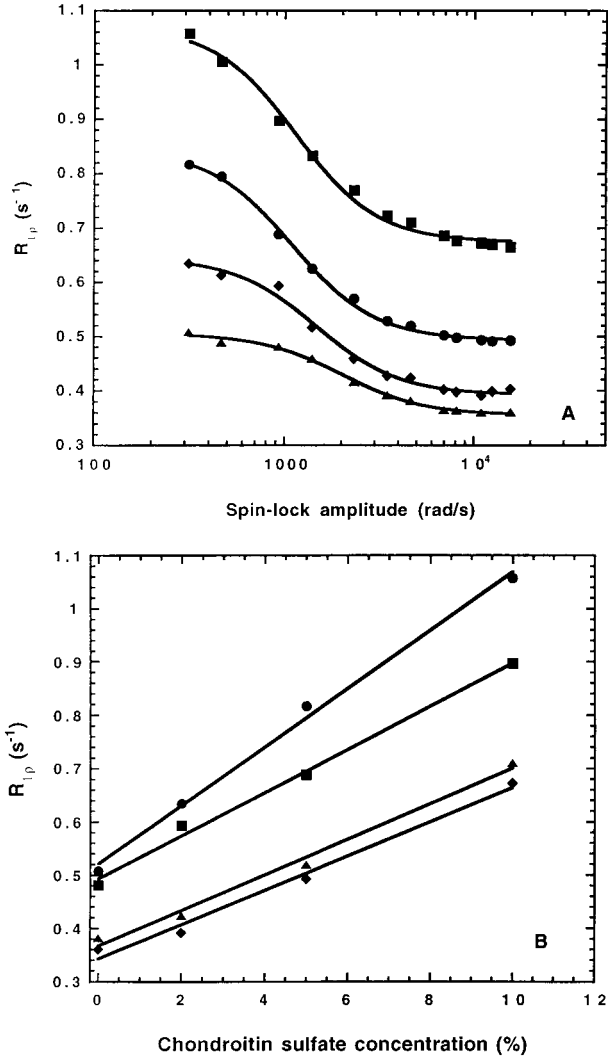

Fig. 2. Dependence of water $R_{1\rho}$ dispersion on CS concentration. (*A*) The dispersion of the buffer (▲) is less than that of 2 (◆), 5 (●), and 10% (■) solutions of CS. The correlation time of these dispersion plots is in agreement with literature values for hydroxyl exchange times, under similar conditions. *B* shows the dependence of $R_{1\rho}$ with CS concentration at various spin-lock amplitudes: 314 rad/s (●), 930 rad/s (■), 4,650 rad/s (▲), and 1.1×10^4 rad/s (◆).

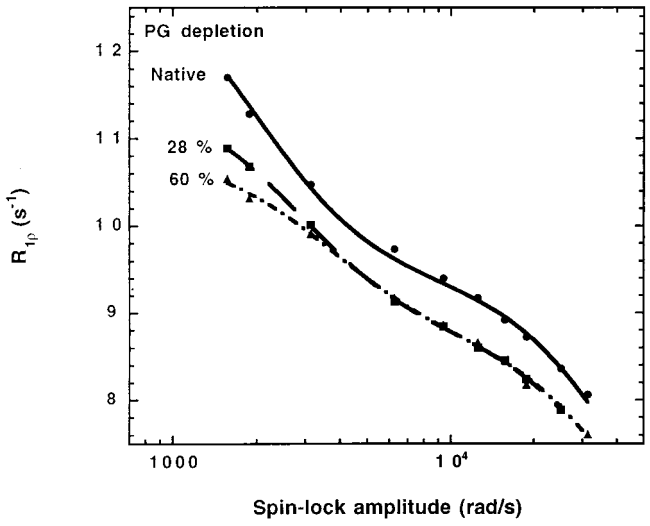

Fig. 3. Dependence of water $R_{1\rho}$ relaxation and dispersion in articular cartilage on PG loss. This figure shows the water dispersion profile of a representative sample of cartilage before (●), after 28% PG depletion (■), and after 60% PG depletion (▲). The error bar of measurement is about 0.5%. Solid lines represent fits to a bi-Lorentzian function. The low frequency dispersion is attributed to proton exchange from NH and OH groups, whereas the high frequency dispersion is the result of the exchange of entire water molecules (see text).

theories to explain the magnetic field dependence of T_1 relaxation (17), including one which proposes the exchange of a small number of well defined water molecules buried inside the protein with the bulk water on a submicrosecond time scale (16). Although this model explains the dispersion of T_1 with field strength, the time scale is too fast to account for low field $T_{1\rho}$ dispersion.

$T_{1\rho}$ measurements are sensitive to slower motions and have been used to investigate the biophysical characteristics of protein solutions and biological tissues (18). However, most of these studies have been performed with spin-locking fields in the 2–30 kHz regime. Knispel *et al.* (9) have shown that a model which invokes a range of correlation times accounted best for the observed dispersion in the 2 kHz to 30 MHz regime, suggesting that several relaxation mechanisms are present in this frequency range. Virta *et al.* (7) found that $T_{1\rho}$ dispersion of protein solutions at low frequency (<8.5 kHz) is sensitive to protein content, denaturation, and cross-linking. A cross-relaxation mechanism by which magnetization is transferred from the protein system to the water by means of a "dipolar energy overlap" was proposed to explain these results (7).

We propose that the proton exchange of labile NH and OH protons with bulk water is a significant contributor to the low frequency $T_{1\rho}$ dispersion in biological systems. There are two elements to this relaxation mechanism. (*i*) The efficient relaxation of the NH and OH protons caused by the fast quadrupolar relaxation of the spin = 1 ^{14}N (19, 20) and spin = 5/2 ^{17}O is mediated by scalar coupling between ^{14}N-^{1}H or ^{17}O-^{1}H and chemical exchange with the bulk water to affect bulk water $T_{1\rho}$ relaxation (15). (*ii*) The proton exchange of the chemically shifted NH/OH moieties with water can also lead to water relaxation (21, 22). The phenomena of chemical exchange and fast quadrupolar relaxation contribute to water proton relaxation through the first mechanism. However, only hydrogen exchange can cause water relaxation through the second mechanism by modulating the chemical shift difference between NH/OH protons and water.

The transverse relaxation of water under the conditions of fast exchange has been given (23).

$$R_2^{\text{obs}} = f_A R_{2A} + f_B R_{2B} + f_A f_B \tau_{ex} \Delta\omega^2, \qquad [2]$$

where R_2^{obs} is the observed relaxation rate; $f_{A,B}$ is the mole fraction of species A and B, $R_{2A,B}$ is the transverse relaxation rate of the species A and B, respectively; τ_{ex} is the chemical exchange time; and $\Delta\omega$ is the chemical shift difference between the sites. An analogous expression has been derived to account for $T_{1\rho}$ relaxation in paramagnetic solutions by Chopra *et al.* (24). In the limit of low spin-lock amplitudes, $T_{1\rho}$ approximates T_2. We can use Eq. **2** to interpret the low frequency $T_{1\rho}$ data presented in this article by using typical values for NH chemical shifts, relaxation times, and concentrations.

We have evaluated the role of proton exchange by studying two relevant systems, smMLCKp, to measure the NH contribution within a peptide system, and CS, to measure the OH contribution from PG. The unblocked smMLCKp provides a

Table 1. The characteristic parameters of the water $R_{1\rho}$ dispersion curve of articular cartilage in 5 separate specimens

Average proteoglycan loss, %	Amplitude of slow component $\times 10^3$, a.u.	Correlation time of slow component, $\times 10^{-6}$ sec***	Amplitude of fast component $\times 10^4$, a.u.	Correlation time of fast component, $\times 10^{-6}$ sec
0	6.1 ± 1.3	443 ± 16	17 ± 6	23 ± 7
39.6	7.0 ± 1.2	387 ± 81	15 ± 6	25 ± 8
57.1	5.8 ± 1.6	353 ± 64	18 ± 2	20 ± 2

The data are reported as mean ± SD. The asterisks indicate that the decrease in the slow correlation time with proteoglycan loss was statistically significant ($P < 0.005$, $r = -0.74$).

meaningful model for NH-mediated water relaxation effects. Each molecule has a total of 54 exchangeable NH protons and only 3 hydroxyl groups (the C-terminal hydroxyl group is deprotonated at experimental conditions) on the peptide, therefore the water $R_{1\rho}$ dispersion of the smMLCKp solution should be dominated by NH-mediated interactions. In contrast, CS has 3 exchangeable hydroxyl protons but only 1 exchangeable NH proton. The OH/NH ratio and the slow exchange of this amide proton [$\sim$25 s^{-1} at pH 7.4 and 22°C (25, 26)] indicate that hydroxyl groups should dominate the water $R_{1\rho}$ dispersion in CS solutions. Thus, the dispersion profiles of these model systems allow us to evaluate separately the effects of amide and hydroxyl exchange on water relaxation (Figs. 1 and 2).

Let us consider the quadrupolar relaxation of natural abundance ^{14}N and ^{17}O nuclei, in the context of amide and hydroxyl group rotations. We assume for the present discussion that the lower limit of the rotational correlation time of NH and OH moieties is roughly equal to that of methyl group rotations in protein solutions, i.e., $\sim$50 ps at 30°C in millimolar solutions (27). As the quadrupole-coupling constant of ^{14}N in amino acids varies between 0.8–3.4 MHz (28), we have used an approximate value of 2.5 MHz. In the fast motion regime, the longitudinal relaxation rate can be estimated as (29)

$$\frac{1}{T_1} = \frac{3\pi^2}{2}\left(1 + \frac{\eta^2}{3}\right)\left(e^2qQ/\hbar\right)^2\tau_r, \qquad [3]$$

where $(e^2qQ/\hbar)$ is the nuclear quadrupole coupling constant, η is the asymmetry parameter, and τ_r is the rotational correlation time. The quadrupole coupling constant has been measured for many quadrupolar nuclei in various molecules and environments. The asymmetry parameter ranges between 0 and 1, providing a minimal contribution to the overall relaxation rate.

We therefore estimate the T_1 of ^{14}N nuclei in NH groups to be $\sim$200 μs (0.1–2 ms, for the range of coupling constant values given previously). The small difference between the ^{15}N-labeled peptide, which does not exhibit quadrupolar relaxation, and the ^{14}N peptide, which does, indicates that quadrupolar relaxation of nitrogen nuclei plays a small role in the low frequency bulk water $T_{1\rho}$ dispersion for this peptide system. We can attribute this to the fact that the T_1 of ^{14}N nuclei is much faster than the proton exchange rate and does not significantly influence the relaxation of the NH protons.

Similarly we can estimate the contribution from quadrupolar relaxation of ^{17}O nuclei in ^{17}O-H groups. The quadrupolar coupling constant of ^{17}O in OH groups in organic compounds is $\sim$9 MHz (30). By using Eq. **3** and the assumptions as above, we estimate the T_1 of ^{17}O in CS to be $\sim$16 μs. This extremely fast relaxation time and the low natural abundance of ^{17}O (0.037%) eliminates the quadrupolar relaxation of ^{17}O nuclei as a substantial relaxation mechanism for water relaxation in both the peptide and CS systems.

Indeed, the isotopic substitution of ^{15}N in the smMLCKp demonstrates that the quadrupolar relaxation of ^{14}N has a relatively minor effect on the water relaxation. Because ^{15}N nuclei do not exhibit quadrupolar relaxation, the dispersion observed in the ^{15}N-labeled peptide solution is attributed to the chemical exchange of N-H protons with the bulk water. Because we have precluded quadrupolar relaxation of ^{17}O from being a significant $T_{1\rho}$ dispersive mechanism, proton exchange of hydroxyl groups remains as the leading dispersive mechanism in CS solutions. Hills and coworkers (31, 32) have demonstrated that the exchange of hydroxyl protons contributes to transverse relaxation of water protons and that T_2 measurements could be used to estimate the proton exchange rate and chemical shift in protein and sugar solutions.

Similarly, we can interpret the $T_{1\rho}$ dispersion data from ^{15}N-peptide solutions by using Eq. **2**. Assuming values of 3 s for the T_2 of pure water, 1.2 s for the T_2 of ^{15}N-H protons in the unstructured peptide (33), a chemical shift difference of 1.8 ppm for the NH protons relative to on-resonance water, an exchange rate of 700 s^{-1} between NH protons and water, and the concentrations presented earlier, we can estimate the observed water T_2 in the peptide solutions. The water T_2 in our peptide solutions is predicted to be $\sim$1 s, whereas that extrapolated from Fig. 1 is 1.5 s. This agreement suggests that proton exchange between chemically shifted species is the dominant mechanism for relaxation in our model systems. In fact, bulk water T_2 is relatively independent of the NH proton T_2 but is dominated by the chemical shift separation, accounting for the small difference in water relaxation observed in ^{14}N- and ^{15}N-peptide solutions.

If we model the effective correlation rate of water dispersion in the peptide solutions to be the sum of the correlation rates of the different relaxation mechanisms, we can give some physical meaning to the measured correlation times. In our case, the individual relaxation mechanisms are (*i*) exchange modulation of chemical shift of the amide protons and (*ii*) exchange modulation of scalar coupling from natural abundance $H_2{}^{17}O$ (15). Assuming that these mechanisms are independent of each other, we can write

$$\tau_{obs}^{-1} = \tau_{NH}^{-1} + \tau_{OH}^{-1}, \qquad [4]$$

where τ_{obs} is the correlation time of the water dispersion curve, and τ_{OH} and τ_{NH} are the correlation times that maximize the spectral density function associated with the OH- and NH-associated relaxation processes, respectively. Because quadrupolar relaxation effects are small, τ_{NH} and τ_{OH} are directly related to the exchange times of the NH and hydroxyl protons with water.

We can evaluate the observed correlation rate of the water dispersion in the peptide and CS solutions by using Eq. **4**. The overall NH to water proton exchange rate for the smMLCKp was calculated according to published methods and determined to be 700 s^{-1} at pH 7.4 and 22°C (25, 26). Briefly, the overall exchange rate is calculated as the weighted sum of the exchange rates from individual NH groups. The exchange rate of each group is calculated as the sum of the acid-, base-, and water-catalyzed rates as determined from previous measurements (25, 26). The

calculated overall exchange rate is in agreement with the literature (34). The correlation rate of buffer dispersion was determined to be 1,100 s^{-1}, which is in agreement with the results of Meiboom (15). Therefore, the correlation rate in our peptide system is predicted to be 1,800 s^{-1} (using Eq. **4**), which is in good agreement with the observed rate of 1,700 s^{-1}.

Similarly, the observed correlation rate in CS solutions, ~1200 s^{-1}, is in good agreement with the results of Hills (32), who reported a proton exchange rate of 1,400 s^{-1} at neutral pH. The observed result that the hydroxyl groups in CS exchange with water with a rate similar to water–water hydrogen exchange at neutral pH [1100 s^{-1} (15)] suggests that the exchange mechanism might be similar.

The bi-Lorentzian shape of the water $R_{1\rho}$ dispersion profile in cartilage indicates that there are at least two distinct dispersive processes in the 0.1–6 kHz frequency range. The low frequency correlation rate increases as the tissue is degraded with trypsin and loses PG, but the high frequency component does not change significantly. The low frequency dispersion component is particularly important for *in vivo* experiments, because this is the range of spin-lock amplitudes that can be achieved on MRI systems.

The measured correlation rate for the low frequency dispersion in cartilage is within 25% of the sum of the peptide and CS correlation rates according to Eq. **4**, suggesting that the slow dispersion component in cartilage is derived from proton exchange of both NH and OH groups with water. The increase in the low frequency correlation rate with PG loss could be the result of increased proton exchange rates. In fact, it has been shown that because of the fixed charge density in cartilage (caused by negatively charged PG molecules), the sodium content is higher in the tissue than in the surrounding fluid as a result of Donnan equilibrium (35). Similar arguments have been used to suggest that cartilage fluid is more acidic than the surrounding environment (36). The loss of PG from the matrix leads to an increase in the basicity of the cartilage fluid component. For our conditions, the cartilage fluid pH should increase from ~7.0 in native tissue to ~7.2 in 60% PG-depleted tissues, using literature values for sodium content in normal and degraded tissues (37, §). This increase in pH would increase the exchange rates from hydroxyl and amide groups 1.6-fold. The slow correlation rate increased by ~26% (Table 1), in agreement with the predicted increase. In fact, the $T_{1\rho}$ dispersion of bovine cartilage in the 0–3 kHz regime has been shown to be pH-sensitive (18), indicating that chemical exchange is responsible for the low field dispersion in cartilage. Leipinsh and Otting (38) reported that proton exchange from amino acids to water, at physiologic conditions, might occur at a range that could very well explain the $T_{1\rho}$ dispersion properties of cartilage.

According to our model, proton exchange seems to be the dominant low frequency $T_{1\rho}$ dispersion mechanism in peptide and CS solutions and cartilage. The proton exchange model accounts for 70% of the effective correlation time of water dispersion profiles in cartilage. Therefore, we propose that hydrogen exchange, between NH groups that are chemically shifted by ~1.8 ppm from water protons and water, contributes heavily to the low frequency water $T_{1\rho}$ dispersion in biological systems.

It should be noted that Eq. **4** provides an empirical model to interpret our observations. Because the correlation times referred to in Eq. **4** are derived from the maximization of a model-dependent spectral density function, the relaxation model used will influence the interpretation of these values. For our description, both the proton exchange rate and the chemical shift difference between the labile groups and water determine the effective correlation time. Proton exchange between NH groups and water depends on several factors, including primary structure and hydrogen bonding. By experiment, we can observe only the overall exchange rate. The distribution of exchange rates from different moieties on the molecules (side chain NH vs. backbone amide, for example) along with the distribution of chemical shift values leads us to interpret the effective correlation times not as exchange times *per se*, but as indicators of proton exchange-induced relaxation.

We have focused the discussion on the low frequency dispersion in cartilage because the range of spin-lock strengths that are useful for diagnostic imaging lie in the 0.1–1.5 kHz regime. We can also offer a plausible interpretation for the higher frequency cartilage dispersion ($\tau \sim 20$ μs) in the context of the current literature. It has been shown that the exchange of entire water molecules between "bound" (i.e., associated with a macromolecule) and "free" sites can be a relaxation mechanism (39). The residence time of water molecules in the hydration layer has been estimated to be ~10 μs in tissue, and water molecules closely associated with the tissue matrix have short relaxation times as a result of motional restriction (40). The higher frequency dispersion component in cartilage may therefore arise from the exchange of entire water molecules, closely associated with the tissue matrix, with the solvent water. This explanation is consistent with the observation that PG loss did not significantly affect the higher frequency dispersion in cartilage, because PG does not have well defined water-binding sites based on magnetization transfer measurements (41).

Our measurements demonstrate the existence of at least two processes that contribute to water dispersion in bovine type II collagen (based on the bi-Lorentzian $T_{1\rho}$ dispersion of collagen solutions). The low frequency dispersion component likely reflects the contribution of proton exchange. The high frequency dispersion is attributed to the exchange of water molecules between bound and free states. Therefore, collagen may also contribute to water $T_{1\rho}$ dispersion in cartilage. We postulate that collagen influences water molecules through collagen–water and collagen–PG interactions. Because of the latter, $T_{1\rho}$ measurements may be sensitive to macromolecular interactions between collagen and PG. At this time, we have not isolated the individual contributions from PG and collagen to bulk water $T_{1\rho}$ dispersion. However, the good correlation obtained between PG loss and low frequency $T_{1\rho}$ dispersion shows that $T_{1\rho}$ is sensitive to cartilage PG content.

The observed correlation between low frequency dispersion and PG loss suggests that $T_{1\rho}$ measurements may be particularly useful for the longitudinal evaluation of cartilage disease, and for noninvasively monitoring the efficacy of therapy (42). A relatively small change in the relaxation or correlation time may produce a noticeable effect in $T_{1\rho}$-weighted images. Because the current measurements are spectroscopic and represent the global effects of trypsin digestion, they should be viewed as the lower limit of the sensitivity of this technique. In fact, trypsin digestion is known to produce a heterogeneous pattern of PG loss, with laminae at the tissue edges having maximal PG loss. Initial imaging experiments show that the effects of PG loss on $T_{1\rho}$ are magnified on $T_{1\rho}$-weighted images, and degradation-induced signal laminae can be observed.¶ Importantly, the correlation time measurements reported here allow us to study the biophysical mechanisms underlying $T_{1\rho}$ relaxation and dispersion in cartilage. These measurements will be useful for developing methods to noninvasively map PG content in cartilage.

§Shapiro, E. M., Borthakur, A., Kaufman, J. H., Kudchodkar, S. B., Kneeland, J. B., Leigh, J. S. & Reddy, R. (2000) *Osteoarthritis Cartilage* **8,** S12 (abstr.).

¶Akella, S. V. S., Regatte, R., Borthakur, A., Shapiro, E., Duvuri, U., Kneeland, J. B., Leigh, J. S. & Reddy, R. (2001) *Proc. Int. Soc. Magn. Reson. Med. (Glasgow, Scotland)* **3,** 2108 (abstr.).

Conclusion

Our data suggest that proton exchange, from NH groups on simple peptide molecules with water, contribute to bulk water $T_{1\rho}$ relaxation in a concentration-dependent fashion. Hydroxyl groups in CS can also contribute. The apparent sensitivity of the low frequency dispersion (in the 0.1–1.5 kHz regime) to PG loss from cartilage suggests that $T_{1\rho}$-based imaging schemes may be used to probe cartilage integrity.

This work was performed at a National Institutes of Health-supported Regional Research Center by National Institutes of Health Grants RR02305 (to J.S.L.), MH11960 (to U.D.), AR45242 (to R.R.), GM81347 (to S.W.E.), and DK39806 (to A.J.W.).

1. Hall, B. K. & Newman, S. (1991) *Cartilage: Molecular Aspects* (CRC, Boca Raton, FL).
2. McCauley, T. R. & Disler, D. G. (1998) *Radiology (Easton, Pa.)* **209,** 629–640.
3. Insko, E. K., Kaufman, J. H., Leigh, J. S. & Reddy, R. (1999) *Magn. Reson. Med.* **41,** 30–34.
4. Bashir, A., Gray, M. L., Hartke, J. & Burstein, D. (1999) *Magn. Reson. Med.* **41,** 857–865.
5. Duvvuri, U., Reddy, R., Patel, S. D., Kaufman, J. H., Kneeland, J. B. & Leigh, J. S. (1997) *Magn. Reson. Med.* **38,** 863–867.
6. Redfield, A. G. (1955) *Phys. Rev.* **98,** 1787–1809.
7. Virta, A., Komu, M. & Kormano, M. (1997) *Magn. Reson. Med.* **37,** 53–57.
8. Sepponen, R. (1992) in *Magnetic Resonance Imaging*, eds. Stark, D. D. & Bradley, W. G. (Mosby, St. Louis), Vol. 1, pp. 204–218.
9. Knispel, R. R., Thompson, R. T. & Pintar, M. M. (1974) *J. Magn. Reson.* **14,** 44–51.
10. Duvvuri, U., Charagundla, S. R., Kudchodkar, S. B., Kaufman, J. H., Kneeland, J. B., Rizi, R., Leigh, J. S. & Reddy, R. (2001) *Radiology (Easton, Pa.)* **220,** 822–826.
11. Rizi, R. R., Charagundla, S. R., Song, H. K., Reddy, R., Stolpen, A. H., Schnall, M. D. & Leigh, J. S. (1998) *J. Magn. Reson. Imaging* **8,** 1090–1096.
12. Lee, A. L., Kinnear, S. A. & Wand, A. J. (2000) *Nat. Struct. Biol.* **7,** 72–77.
13. Farndale, R. W., Sayers, C. A. & Barrett, A. J. (1982) *Connect. Tissue Res.* **9,** 247–248.
14. Bank, R. A., Krikken, M., Beekman, B., Stoop, R., Maroudas, A., Lafeber, F. P. & te Koppele, J. M. (1997) *Matrix Biol.* **16,** 233–243.
15. Meiboom, S. (1965) *J. Chem. Phys.* **34,** 375–388.
16. Venu, K., Denisov, V. P. & Halle, B. (1997) *J. Am. Chem. Soc.* **119,** 3122–3134.
17. Bryant, R. G. (1996) *Annu. Rev. Biophys. Biomol. Struct.* **25,** 29–53.
18. Chen, E.-L. (1998) Ph.D. thesis (Univ. of Pennsylvania, Philadelphia).
19. Solomon, I. (1959) *C. R. Acad. Sci. (Paris)* **248,** 92–94.
20. Solomon, I. (1959) *C. R. Acad. Sci. (Paris)* **248,** 1631–1632.
21. Hills, B. P. (1992) *Mol. Phys.* **76,** 509–523.
22. Hills, B. P. (1992) *Mol. Phys.* **76,** 489–508.
23. McLaughlin, A. C. & Leigh, J. S. (1973) *J. Magn. Reson.* **9,** 296–304.
24. Chopra, S., McClung, R. E. D. & Jordan, R. B. (1984) *J. Magn. Reson.* **59,** 361–372.
25. Bai, Y., Milne, J. S., Mayne, L. & Englander, S. W. (1993) *Proteins* **17,** 75–86.
26. Connelly, G. P., Bai, Y., Jeng, M.-F. & Englander, S. W. (1993) *Proteins* **17,** 87–92.
27. Lee, A. L., Flynn, P. F. & Wand, A. J. (1999) *J. Am. Chem. Soc.* **121,** 2891–2902.
28. Hunt, M. J. & Mackay, A. L. (1976) *J. Magn. Reson.* **22,** 295–301.
29. Abragam, A. (1961) *The Principles of Nuclear Magnetism* (Clarendon, Oxford).
30. Hsieh, Y., Koo, J. C. & Hahn, E. L. (1972) *Chem. Phys. Lett.* **13,** 563–566.
31. Hills, B. P., Wright, K. M. & Belton, P. S. (1989) *Mol. Phys.* **67,** 1309–1326.
32. Hills, B. P. (1991) *Mol. Phys.* **72,** 1099–1121.
33. Cavanagh, J., Fairbrother, W. J., Palmer, A. G., III, & Skelton, N. J. (1996) *Protein NMR Spectroscopy: Principles and Practice* (Academic, San Diego).
34. Ehrhardt, M. R., Urbauer, J. L. & Wand, A. J. (1995) *Biochemistry* **34,** 2731–2738.
35. Lesperance, L. M., Gray, M. L. & Burstein, D. (1992) *J. Orthop. Res.* **10,** 1–13.
36. Kaufman, J. H. (2000) Ph.D. thesis (Univ. of Pennsylvania, Philadelphia).
37. Shapiro, E. M., Borthakur, A., Dandora, R., Kriss, A., Leigh, J. S. & Reddy, R. (2000) *J. Magn. Reson.* **142,** 24–31.
38. Leipinsh, E. & Otting, G. (1996) *Magn. Reson. Med.* **35,** 30–42.
39. Koening, S. H., Hallenga, K. & Shporer, M. (1975) *Proc. Natl. Acad. Sci. USA* **72,** 2667–2671.
40. Diegel, J. G. & Pintar, M. M. (1975) *Biophys. J.* **15,** 855–860.
41. Kim, D. K., Ceckler, T. L., Hascall, V. C., Calabro, A. & Balaban, R. S. (1993) *Magn. Reson. Med.* **29,** 211–215.
42. Potter, K., Buttler, J. J., Horton, W. E. & Spencer, R. G. S. (2000) *Arthritis Rheum.* **43,** 1580–1590.